pollutants

MDPI

Article

Electrochemical Anodic Oxidation Treatment of Pool Water Containing Cyanuric Acid

Jaime Carbajo [1], Jefferson E. Silveira [2], Inês Gomes [3,4], Annabel Fernandes [3,4,*], Lurdes Ciríaco [3,4], Alicia L. García-Costa [2], Juan A. Zazo [2] and Jose A. Casas [2]

[1] Chemical and Materials Engineering Department, Universidad Complutense de Madrid, Pl. de las Ciencias, 2, 28040 Madrid, Spain; jaime.carbajo@ucm.es
[2] Chemical Engineering Department, Universidad Autonoma de Madrid, Ctra. Colmenar km. 15, 28049 Madrid, Spain; jefferson.silveira@uam.es (J.E.S.); alicial.garcia@uam.es (A.L.G.-C.); juan.zazo@uam.es (J.A.Z.); jose.casas@uam.es (J.A.C.)
[3] FibEnTech-UBI, Universidade da Beira Interior, 6201-001 Covilhã, Portugal; ines.margarida.gomes@ubi.pt (I.G.); lciriaco@ubi.pt (L.C.)
[4] Department of Chemistry, Universidade da Beira Interior, 6201-001 Covilhã, Portugal
* Correspondence: annabelf@ubi.pt

Abstract

Cyanuric acid (CYA) is widely used as a chlorine stabilizer in swimming pools, but concentrations above 75 mg L^{-1} cause overstabilization and loss of disinfection capacity. This study evaluated CYA removal by advanced oxidation processes, including heterogeneous photocatalysis, photo-Fenton, photo-persulfate, and anodic oxidation (AO). AO with boron-doped diamond anodes proved most effective, achieving up to 90% total organic carbon removal in ultrapure water. When applied to real swimming pool samples (118 and 251 mg L^{-1} CYA), the process achieved significant CYA abatement, demonstrating its potential as a practical strategy to control overstabilization without additional chemicals.

Keywords: cyanuric acid; dichloroisocyanuric acid; advanced oxidation processes; electrochemical oxidation; swimming pool water

check for updates

Academic Editor: Flavio Rodrigues

Received: 11 May 2025
Revised: 12 September 2025
Accepted: 22 October 2025
Published: 3 November 2025

Citation: Carbajo, J.; Silveira, J.E.; Gomes, I.; Fernandes, A.; Ciríaco, L.; García-Costa, A.L.; Zazo, J.A.; Casas, J.A. Electrochemical Anodic Oxidation Treatment of Pool Water Containing Cyanuric Acid. *Pollutants* **2025**, *5*, 39. https://doi.org/10.3390/pollutants5040039

Copyright: © 2025 by the authors. Licensee MDPI, Basel, Switzerland. This article is an open access article distributed under the terms and conditions of the Creative Commons Attribution (CC BY) license (https://creativecommons.org/licenses/by/4.0/).

1. Introduction

Recreational waters are widely recognized as potential sources of human illness. Exposure to microbial pathogens in these environments has been linked to a broad spectrum of adverse health outcomes, most notably gastrointestinal infections, but also respiratory, dermatological, and otic diseases [1].

Free chlorine (OCl^- or HOCl) acts as an efficient barrier to the transmission of pathogens, being the most widely used disinfectant in recreational water due to its low cost and efficacy to inactivate most of the pathogens within minutes, even at low concentrations (i.e., 1–2 ppm free available chlorine) [2–4]. However, HOCl is particularly unstable and is rapidly decomposed into Cl^- by UV radiation. To prevent the rapid loss of hypochlorite, cyanuric acid (CYA) has been used in recent decades as a chlorine stabilizer. CYA presents low solubility in water, being a stable weak acid in aqueous solution (pKa1 = 7.0, pKa2 = 11.3, and pKa3 = 14.5). In aqueous medium, it is present as a mixture of tautomers (Figure 1), with the keto form 2,4,6-trioxo-s-triazine (pH < 6) and the enolic form 2,4,6-trihydroxy-s-triazine (cyanuric acid, pH > 6) [5,6].

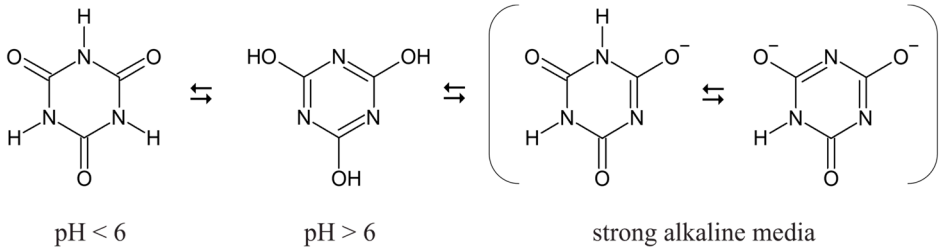


Figure 1. Cyanuric acid tautomers (adapted from [6]).

In the presence of free chlorine, CYA is in equilibrium with its chlorinated cyanurate, dichloroisocyanuric acid (DCC), as described in Figure 2. This reversible CYA-chlorine equilibrium regulates the amount of free chlorine, avoiding fast chlorine sunlight degradation.

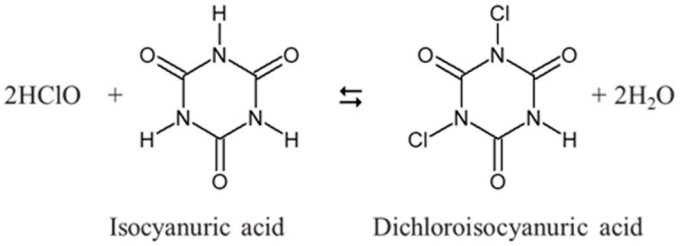


Figure 2. Free chlorine, cyanuric acid, and chlorinated cyanurate equilibria.

Although cyanuric acid has proven to be a very effective free chlorine stabilizer, its concentration should be kept in a relatively narrow range, between 30–50 mg L^{-1}, to be effective, and should not exceed 75 mg L^{-1} [7,8]. At lower concentrations (i.e., <30 mg L^{-1}), there is too much free chlorine, being rapidly decomposed by sunlight. Contrarywise, overstabilization occurs when CYA concentration exceeds 75 mg L^{-1} and the equilibrium shifts towards DCC formation, reducing free chlorine to an extent where its biocidal effect is severely limited [9].

As of today, the only viable solution to maintain CYA levels in the appropriate concentration is the continuous or periodic replacement of the pool's water. This method is time-consuming, costly, and environmentally unsustainable, if not prohibited in areas with severe water scarcity. Therefore, the development of an effective method to remove CYA from recreational water matrices could lead to considerable water savings. Different strategies have been proposed for the removal of CYA from swimming pool water. Bobadilla et al. [10] suggested precipitation with melamine, obtaining only partial removal and undesired side effects such as turbidity and coloration. Photocatalytic degradation with TiO_2/fluoride required long reaction times under acidic conditions, which limits its applicability [11]. Ozonation has also been investigated, but efficiency and operational costs remain important constraints [12]. Taken together, these studies illustrate the challenges associated with CYA removal and underline the need to explore alternative approaches.

Despite extensive efforts to date, no practical method has been established for controlling cyanuric acid concentration in recreational waters. The present study explores the feasibility of degrading CYA by different advanced oxidation processes, namely heterogeneous photocatalysis, photo-Fenton, photo-persulfate, and anodic oxidation. Finally, the CYA removal is evaluated in real swimming pool water subjected to an episode of overstabilization, demonstrating that anodic oxidation may be considered a novel approach for CYA removal in real pool water without chemical addition.

2. Materials and Methods

2.1. Heterogeneous Photocatalysis, Photo-Fenton, and Photo-Persulfate Experiments

Heterogeneous photocatalysis (HPhCat), photo-Fenton (Ph-F), and photo-persulfate (Ph-PS) experiments were carried out using an aqueous CYA solution (50 mg L^{-1}) prepared with ultrapure water obtained from a Milli-Q Advantage A10 purification system (Merck Millipore, Rahway, NJ, USA; 18.2 MΩ cm at 25 °C).

The reactions were performed in a custom-built immersion-wall batch jacketed photoreactor (useful volume: 750 mL; inner diameter: 0.15 m) constructed at the laboratory, equipped with a 150 W medium-pressure Hg lamp (TQ-150, Heraeus, Hanau, Germany), emitting in the 200–600 nm range, with a UV irradiance of 30 W m^{-2} measured by a broad-range photoradiometer (Delta Ohm HD 2102.1, Caselle di Selvazzano (PD), Italy). The lamp was positioned inside a water-cooled quartz tube (outer diameter: 0.04 m). Temperature was controlled between 25 and 90 °C using a thermostatic recirculation system (Huber, Berching, Germany). Experimental conditions for the different assays are summarized in Table 1.

Table 1. Experimental conditions applied in the degradation experiments.

Solution	[CYA] (mg L^{-1})	Process	Experimental Conditions
CYA aqueous solution	50	Heterogeneous photocatalysis	$[TiO_2]$ = 0.5 g L^{-1}; pH_0 = 6.7; T = 25 °C; V = 750 mL; t = 240 min
		Photo-Fenton	$[H_2O_2]_0$ = Stoichiometric; pH_0 = 3; $[Fe^{2+}]_0$ = 10 mg L^{-1}; T = 25 and 90 °C; V = 750 mL; t = 240 min
		Photo-persulfate	$[PS]_0$ = Stoichiometric; T = 90 °C; pH_0 = 6.7; V = 750 mL; t = 240 min
		Anodic oxidation	AO experiments set 1: Anode: DSA or BDD—25 cm^2; Cathode: Stainless steel—25 cm^2; Applied current density = 40 mA cm^{-2}; [NaCl] = 4 g L^{-1}; pH_0 = 6.7; V = 250 mL; t = 240 min for DSA and 60 min for BDD
			AO experiments set 2: Anode: BDD—25 cm^2; Cathode: Stainless steel—25 cm^2; Applied current density = 10, 30 and 40 mA cm^{-2}; [NaCl] = 0.25, 0.5, and 4 g L^{-1}; pH_0 = 6.7; V = 250 mL; t = 60 min
Real swimming pool water	118	Anodic oxidation	Anode: BDD—25 cm^2; Cathode: Stainless steel—25 cm^2; Applied current density = 10, 30 and 40 mA cm^{-2}; pH_0 = 7.2; V = 250 mL; t = 120 min
	251		Anode: BDD—25 cm^2; Cathode: Stainless steel—25 cm^2; Applied current density = 40 mA cm^{-2}; pH_0 = 7.0; V = 250 mL; t = 240 min

In the photo-Fenton experiments, the pH was adjusted with HCl and, once the target temperature was reached, the stoichiometric dose of H_2O_2 (2.12 g/g COD) was added before switching on the lamp. In the photo-persulfate experiments, persulfate (12 g/g COD) was added under the same conditions. For heterogeneous photocatalysis, TiO_2 P25 was added at 0.5 g L^{-1} before irradiation. Electrochemical oxidation experiments in ultrapure water were performed in triplicate. Chemicals were purchased from Sigma-Aldrich (St. Louis, MO, USA), except for persulfate, which was obtained from Panreac (Barcelona, Spain).

2.2. Anodic Oxidation Experiments

All electrochemical assays were performed in a jacketed electrochemical cell, at 20 °C, connected to a DC power supply (FA-2030, Instrutherm, São Paulo, Brazil) and placed on a magnetic stirrer at 300 rpm.

The anodic oxidation (AO) of CYA aqueous solution 50 mg L^{-1} comprised two sets of experiments. In the first set (AO experiments set 1), the influence of anode material on the CYA degradation was assessed. A dimensionally stable anode (DSA), Ti/IrO_2-TaO_2 (Ir/Ta weight ratio 70/30, purchased from UTron Technology Co., Ltd., Xi'an, Shaanxi, China), and a boron-doped diamond (BDD) anode (NeoCoat SA, La Chaux-de-Fonds, Switzerland) were utilized, together with a stainless steel cathode. The gap between the electrodes was set to 0.5 cm. In a second set of anodic oxidation experiments (AO experiments set 2), the influence of applied current density and NaCl concentration on CYA degradation by the BDD anode was assessed. The studied current densities and NaCl concentrations were chosen considering both preliminary tests and the need to balance treatment efficiency with operational cost. Current densities of 10, 30, and 40 mA cm^{-2} represent low, medium, and high operational ranges typically reported in the literature for BDD-based oxidation processes, allowing for assessing both energy efficiency and degradation performance. NaCl concentrations of 0.25, 0.5, and 4 g L^{-1} were selected to evaluate the influence of low-to-high chloride availability on active chlorine generation, while remaining within ranges compatible with pool water chemistry.

AO experiments with real swimming pool water utilized two samples with different CYA concentrations, collected from real operational pools located in the Madrid region, Spain, without further treatment. Sample 1 contained 118 mg L^{-1} CYA and 66.5 mg L^{-1} of total organic carbon (TOC), while sample 2 contained 251 mg L^{-1} CYA and 85.5 mg L^{-1} TOC. Upon arrival at the laboratory, the samples were immediately analyzed for pH, conductivity, carbon and nitrogen content, and chlorine, and were then stored under refrigeration (4 °C) and used within 5 days. Experiments were run with the BDD anode, and the influence of applied current density on AO performance was evaluated.

All the experiments were performed in triplicate. Table 1 presents the experimental conditions for the different AO experiments performed.

2.3. Voltammetric Study

Voltammetry assays of aqueous solutions of two supporting electrolytes, Na_2SO_4 and NaCl, at a concentration of 5 g L^{-1}, without and with CYA 50 mg L^{-1}, were performed in a conventional one-compartment three-electrode electrolytic cell, composed of a boron-doped diamond (BDD, 1 cm^2) working electrode, an Ag/AgCl reference electrode, and a platinum (1 cm^2) auxiliary electrode. Cyclic voltammetry was run at a Potentiostat-Galvanostat Autolab B.V. equipment with NOVA 1.10 (2013) software (Reference 3526 KM Utrecht), purchased from Dias de Sousa S.A. (Alcochete, Portugal). Various potential ranges (−0.5 to 0.5 V; −1 to 1 V; −1.5 to 1.5 V; −2 to 2 V; −2.5 to 2.5 V; and −3 to 3 V), using two sweeping rates for each interval, 10 and 100 mV s^{-1}, at different pH values (5, 8, and 12), were evaluated.

2.4. Analytical Methods

TOC, inorganic carbon, and total nitrogen (TN) were measured using a Shimadzu TOC-VCPH analyzer with a TNM-1 unit (Duisburg, Germany). CYA and DCC concentrations were determined by high-performance liquid chromatography (HPLC) on a Shimadzu Prominence-I LC-2030 C LT system with a diode array detector (Duisburg, Germany) and a C18 column (Eclipse Plus C18, 150 × 4.6 mm, 5 μm, from Agilent Technologies, Santa Clara, CA, USA) operated at 348 K. The mobile phase consisted of a phosphate buffer at pH 7.3

(6.25 mM NaH_2PO_4 and 12.5 mM Na_2HPO_4) with a flow rate of 1 mL min^{-1}. Detection was performed at 213 nm. Nitrate and nitrite were analyzed by ion chromatography (Metrohm 883 IC, Madrid, Spain) with conductivity detection, using a Metrosep A Supp 5 column (250 × 4 mm, from Metrohm AG, Herisau, Switzerland) and an aqueous mobile phase of 3.2 mM Na_2CO_3 and 1 mM $NaHCO_3$ at 0.7 mL min^{-1}. Ammonium was quantified by ion chromatography with chemical suppression (Metrohm 790 IC, Madrid, Spain) coupled to a conductivity detector, employing an aqueous mobile phase of 1.7 mM HNO_3 and 0.7 mM $C_7H_5NO_4$ at a flow rate of 0.7 mL min^{-1}. Test strips (Nº 1272/20228 CE) were used to determine free chlorine.

3. Results and Discussion

3.1. CYA Degradation by Advanced Oxidation Processes

CYA degradation was first evaluated using different advanced oxidation processes, including heterogeneous photocatalysis, photo-Fenton, photo-persulfate, and anodic oxidation (AO experiments set 1, Table 1). Figure 3 shows the results obtained for CYA degradation under these conditions. Heterogeneous photocatalysis, photo-Fenton, and photo-persulfate resulted in negligible CYA or TOC removal. These results confirm the refractory behavior of cyanuric acid observed in the treatment of different chloro-s-triazine herbicides, such as atrazine or simazine, by photocatalyst [13–15], photoelectrocatalysis [16,17], and Fenton or photo-Fenton [18,19]. Photo-Fenton intensification by high temperature (up to 90 °C) was also assessed. Although this intensification approach has proven to be very effective in refractory waters [20,21], it was ineffective with CYA, which seems to present oxidative resistance to hydroxyl radical ($HO^{\bullet}$), regardless of the concentration of radicals formed. According to some authors, the addition of $HO^{\bullet}$ to the CYA ring does occur, but the adduct rapidly loses the $HO^{\bullet}$ in a reversible process [22], explaining why processes relying uniquely on $HO^{\bullet}$ as the oxidant fail to achieve significant CYA removal. Conversely, anodic oxidation led to an effective removal of CYA and TOC, particularly when the BDD anode was used, reaching over 90% TOC mineralization in only 1 h. AO couples the generation of physisorbed $HO^{\bullet}$ at the electrode surface with mediated oxidation by active chlorine species (e.g., HOCl, $Cl^{\bullet}$) using NaCl as electrolyte. Thus, the combination of hydroxyl radicals formed on the surface and the chlorinated active species could explain the greater effectiveness in breaking the triazine ring structure. Accordingly, electrochemical oxidation could be initiated when chlorine reacts with CYA to form DCC, which may be further oxidized by hydroxyl radicals through the triazine ring opening into lower molecular weight organic by-products until their complete mineralization into CO_2 [21]. Attending to the obtained results, anodic oxidation was chosen to evaluate CYA degradation in real recreational waters.

3.2. Voltammetric Study

Figure 4 compares the voltammograms of Na_2SO_4 and Na_2SO_4 + CYA solutions. An anodic peak near 0.75 V and the corresponding cathodic peak were observed, consistent with a reversible redox process. Pei et al. [13] attributed this signal to the interconversion between CYA and dehydrocyanuric acid. The reversibility of this peak indicates that ring opening does not occur at these relatively low potentials, since such a process would not be reversible. In the presence of CYA, the voltammogram exhibited a higher current intensity at potentials close to the oxygen evolution region, suggesting a competition between water oxidation and CYA oxidation, the latter involving more extensive modification of the molecule.

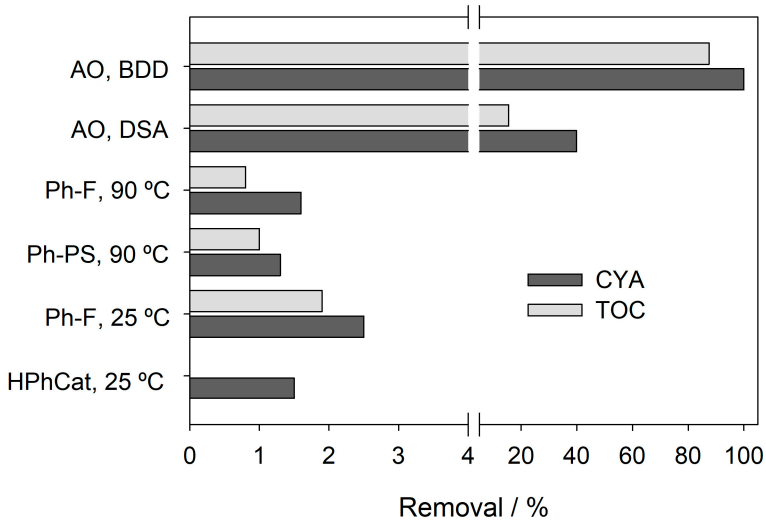


Figure 3. TOC and CYA removals obtained by the different advanced oxidation processes evaluated at the experimental conditions presented in Table 1. AO: Anodic oxidation; Ph-F: Photo-Fenton; Ph-PS: Persulfate; HPhCat: Heterogeneous photocatalysis.

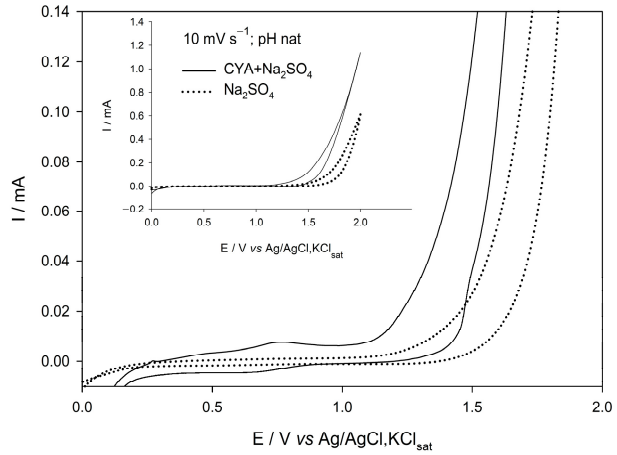


Figure 4. Voltammograms of Na_2SO_4 and Na_2SO_4 + CYA solutions. [CYA] = 50 mg L^{-1}; [Na_2SO_4] = 5 g L^{-1}; natural pH; scanning rate = 10 mV s^{-1}.

Figure 5 presents the voltammograms of the NaCl and NaCl + CYA solutions at different pH values. It can be observed that, at acidic pH, the current intensity in the NaCl solution increases at a lower potential, which may be related to the Cl_2 evolution reaction, by chloride oxidation. This result indicates that, at this pH, chloride oxidation appears to be favored over CYA oxidation.

For the voltammograms at higher pH, both solutions present a similar response. The oxidation of Cl^- to Cl_2 may be delayed in the presence of cyanuric acid by the formation of organochlorine species. In any case, the CYA oxidation will always have as competitive/parallel reactions the evolution reactions of O_2 and Cl_2, in addition to the oxidation of possible organochlorine intermediates, formed in the meantime. Polcaro et al. [23] concluded that a pH between 7–8 would be the most favorable for CYA anodic oxidation. According to these authors, a possible explanation could be the variation with the pH of the reactivity of the organic compound or of the hydroxyl radical. Cyanuric acid has different tautomeric forms, depending on the pH, with pKa values of 6.9, 11.4, and 13.5, with the enol form being less stable than the keto form [24]. Thus, the trend observed in the voltammograms may be related to an increase in the reactivity of cyanuric acid with pH or a reduction in the oxidative power of the hydroxyl radical with the increase in pH.

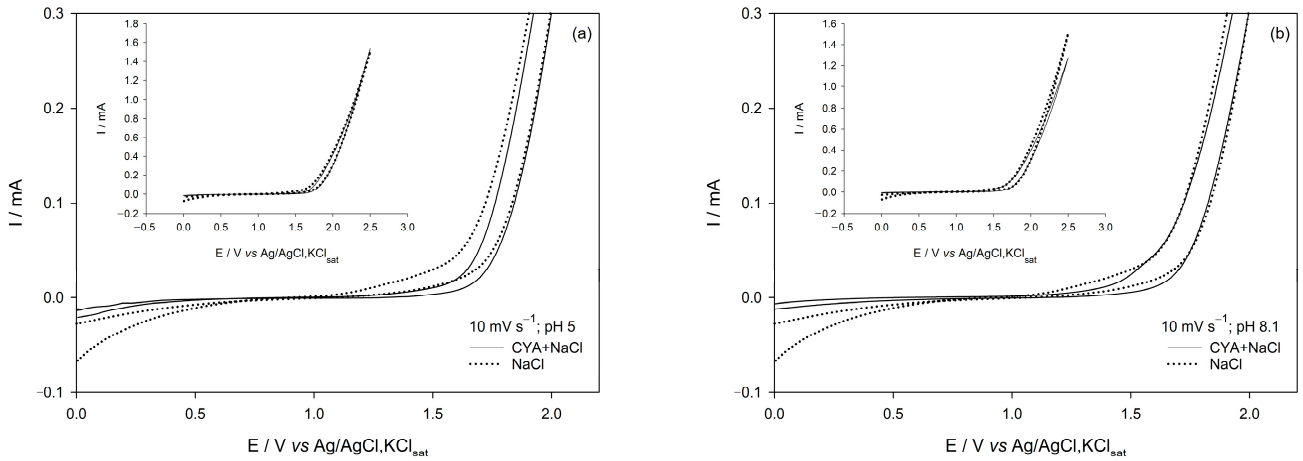


Figure 5. Voltammograms of NaCl and NaCl + CYA solutions. [CYA] = 50 mg L^{-1}; [NaCl] = 5 g L^{-1}; scanning rate = 10 mV s^{-1}; (**a**) pH = 5; (**b**) pH = 8.1 (natural).

3.3. Influence of Operational Parameters on CYA Anodic Oxidation

As anodic oxidation with a BDD anode presented the best results (Figure 3), the influence of applied current density and electrolyte concentration on CYA degradation was assessed (AO experiments set 2, Table 1). An increase in applied current density led to a higher CYA degradation rate (Figure 6a), since CYA degradation may occur by direct oxidation at the anode surface through hydroxyl radicals, whose formation is directly dependent on the applied current density, or by indirect oxidation through chlorine reactive species.

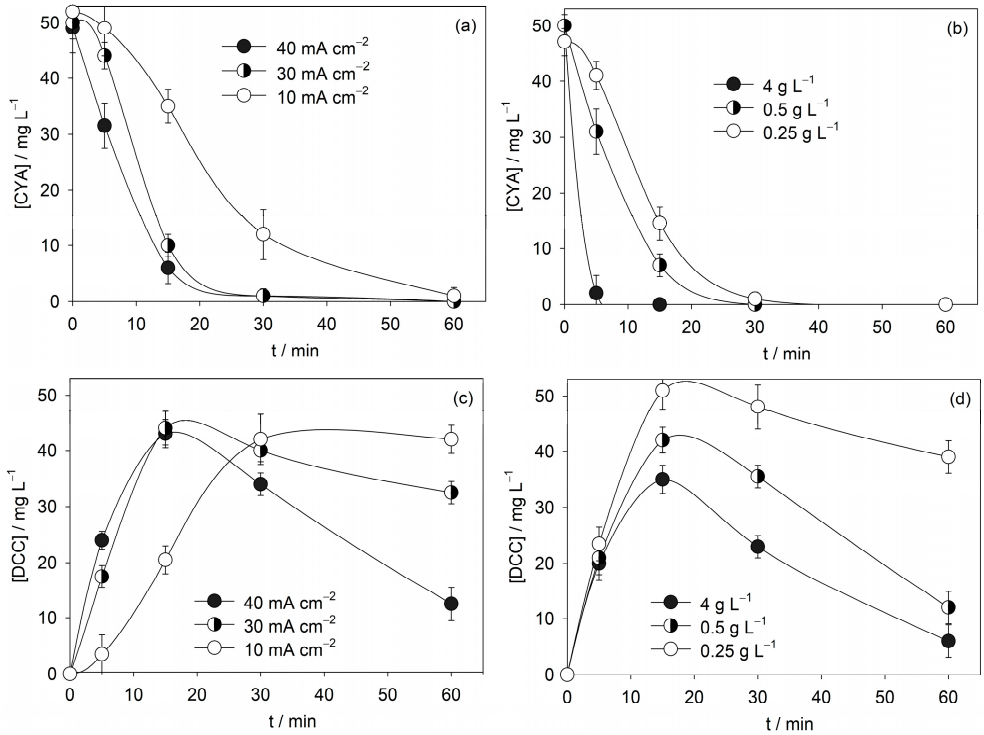


Figure 6. Effect of current density (**a**,**c**) and NaCl concentration (**b**,**d**) on CYA and DCC concentration for the CYA anodic oxidation with BDD anode in ultrapure water. (**a**,**c**) [NaCl] = 0.5 g L^{-1}; (**b**,**d**) Applied current density = 40 mA cm^{-2}.

The importance of hydroxyl radicals and active chlorine species combination in the oxidation mechanism is evident in Figure 6c, with a delayed formation of DCC in the experiments performed at the lowest applied current density. Consequently, higher current

densities promote the generation of both surface-bound HO• radicals and chlorine active species, thereby accelerating CYA degradation and TOC mineralization.

Regarding the influence of the electrolyte concentration, CYA and DCC degradation (Figure 6b,d, respectively) increased with NaCl concentration. After 5 min of experiments, CYA concentration in the solution varies deeply with electrolyte concentration, although DCC concentration is more or less the same. This means that the chloride excess is being used to oxidize DCC, especially at 4 g L^{-1} NaCl. After 15 min, DCC concentration starts to decrease with a similar decay rate to that for 0.5 and 4 g L^{-1}. The formation of DCC as the main oxidation by-product (Figure 6c,d) seems to confirm that oxidation begins with the reaction of chlorine with CYA, forming DCC, which can be further oxidized through the triazine ring opening into lower molecular weight by-products until its complete mineralization into CO_2.

Figure 7 presents TOC, TN, and nitrate-nitrogen concentrations after 60 min of the AO experiments run at different current densities and electrolyte concentrations.

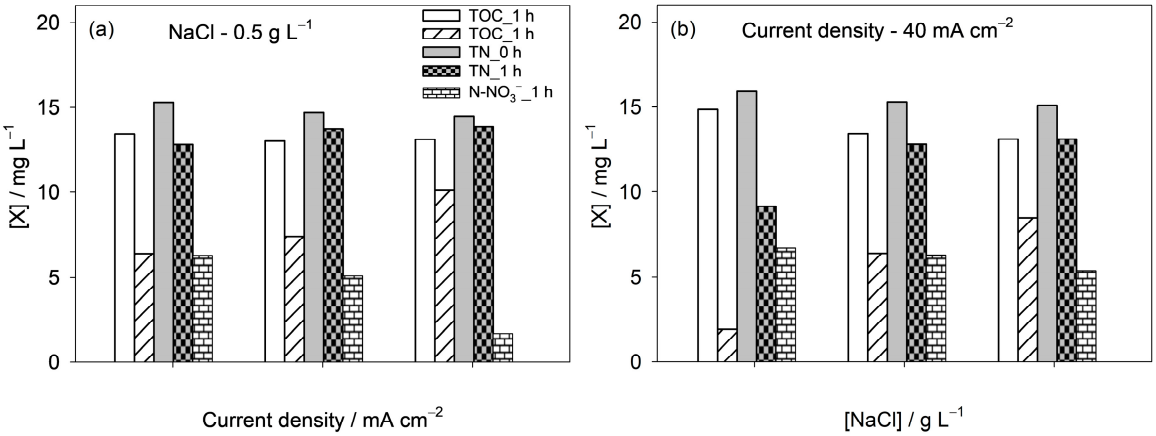


Figure 7. Effect of current density (**a**) and NaCl concentration (**b**) on TOC, TN, and nitrate-nitrogen concentrations after 60 min of CYA anodic oxidation with BDD anode in ultrapure water. (**a**) [NaCl] = 0.5 g L^{-1}; (**b**) Applied current density = 40 mA cm^{-2}.

TOC removal increased with applied current density (23%, 42%, and 52% for 10, 30, and 40 mA cm^{-2}, respectively), probably due to the higher formation of hydroxyl radicals [20]. Conversely, this increase in applied current had little effect on TN removal and increased the formation of nitrate. Regarding the influence of electrolyte concentration, its increase led to increased TOC removal (35%, 52%, and 87% for NaCl concentrations of 0.25, 0.5, and 4 g L^{-1}, respectively), due to the oxidation by the chlorine active species. The increase in formation of these species also led to an increase in TN removal, presenting a smaller effect on the nitrate formation. Table 2 presents TN, N-NO_3^-, N-NO_2^-, and N-NH_4^+ concentrations after 60 min of AO at 0.5 and 4 g L^{-1} NaCl, allowing the determination of the organic nitrogen in solution as well as the gaseous nitrogen formed. At the lowest electrolyte concentration (0.5 g L^{-1}), 2.7 mg L^{-1} of total nitrogen was converted into gaseous forms of nitrogen, and 6 mg L^{-1} remained in solution in the form of organic nitrogen, as DCC and urea. At 4 g L^{-1} NaCl, 6.7 mg L^{-1} of total nitrogen were converted into nitrogen gaseous forms, and 2 mg L^{-1} remained in organic form. This difference shows the importance of utilizing the appropriate amount of electrolyte, depending on the objective of the treatment [24]. The results presented in Table 2 indicate that the nitrogen bound in the triazine ring is primarily converted to nitrate, while smaller fractions are detected as NH_4^+ and trace amounts of NO_2^-. A significant portion is also released as gaseous nitrogen species. This behavior is consistent with a sequential pathway where CYA

is first chlorinated to DCC by electrogenerated HOCl (Equation (1)), followed by oxidative ring cleavage mediated by $^{\bullet}$OH attack (Equation (2)).

$$C_3H_3N_3O_3 + 2HOCl \rightarrow C_3HCl_2N_3O_3 + 2H_2O, \quad (1)$$

$$C_3HCl_2N_3O_3 + OH^{\bullet} \rightarrow NO_3^- + \frac{1}{2}N_2 + 2Cl^- + 3CO_2, \quad (2)$$

Table 2. Total nitrogen, nitrate-, nitrite-, and ammonium- nitrogen concentrations after 60 min of CYA anodic oxidation with BDD anode in ultrapure water. Applied current density = 40 mA cm^{-2}.

[NaCl]/g L^{-1}	TN_0/mg L^{-1}	TN_{final}/mg L^{-1}	N-$NO_3^-{}_{final}$/mg L^{-1}	N-$NO_2^-{}_{final}$/mg L^{-1}	N-$NH_4^+{}_{final}$/mg L^{-1}
0.5	15.3	12.8	6.3	0.1	0.8
4	15.9	9.2	6.7	0.1	0.4

3.4. CYA Anodic Oxidation in Swimming Pool Waters

Anodic oxidation with BDD electrodes was evaluated using two real pool water samples (Table 3). Figure 8a shows the effect of current density on the degradation of water containing 118 mg L^{-1} CYA (Sample 1). After 120 min, CYA removal reached 17% at 10 mA cm^{-2}, 30% at 30 mA cm^{-2}, and 45% at 40 mA cm^{-2}, accompanied by a 58% decrease in TOC at the highest current density. The corresponding pseudo-first-order rate constants (k_{app}) were 2.76, 4.40, and 9.10 × 10^{-3} min^{-1}, confirming the strong dependence of the process on applied current.

Table 3. Characterization of the pool water samples utilized in the study, before and after AO with BDD. Applied current density = 40 mA cm^{-2}.

Pool Water Parameters	Sample 1		Sample 2	
	Before Treatment	After 2-h Treatment	Before Treatment	After 4-h Treatment
CYA/mg L^{-1}	118	65	251	155
TOC/mg L^{-1}	66.5	28.1	85.5	52.1
Inorganic carbon/mg L^{-1}	2.2	1.1	3.2	1.2
pH	7.2	6.9	7.0	6.6
Conductivity/μS cm^{-1}	632	743	1234	1432
NO_3^-/mg L^{-1}	13	75	16	97
NH_4^+/mg L^{-1}	3.5	5.1	3.0	5.0
NO_2^-/mg L^{-1}	≤1	≤1	≤1	≤1
Free chlorine/mg L^{-1}	≤1	3.4	≤1	5.1
Total chlorine/mg L^{-1}	≤1	4.1	≤1	5.4

Figure 8b presents the results for the sample with 251 mg L^{-1} CYA (Sample 2), treated at 40 mA cm^{-2}. In this case, CYA removal was 38% after 240 min, with a k_{app} of 2.25 × 10^{-3} min^{-1}. This constant is about four times lower than in the previous case, reflecting the inhibitory effect of the higher CYA load and organic matter present in real water matrices, which increases competition for oxidants and delays mineralization, in line with the transient accumulation of DCC.

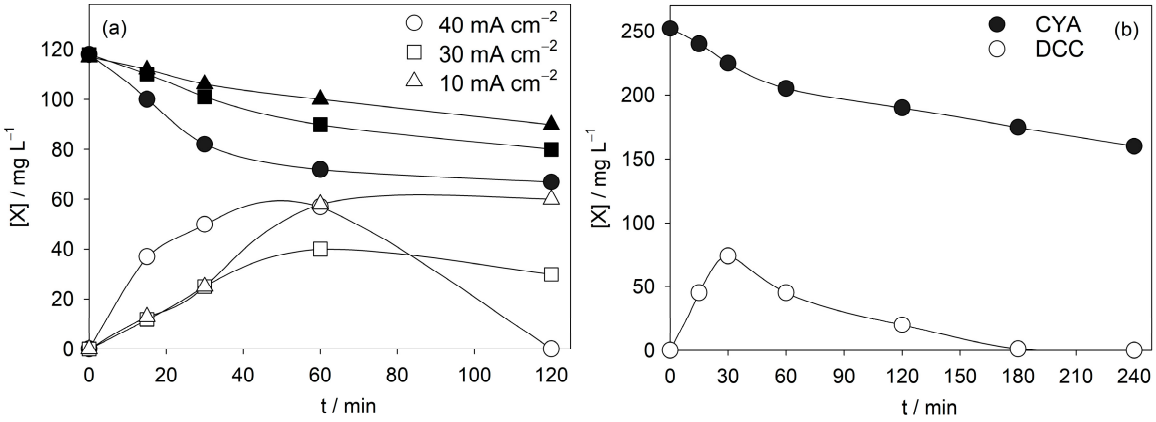


Figure 8. (**a**) Effect of current density on CYA and DCC concentration at anodic oxidation with BDD anode of real swimming pool water with $[CYA]_0$ = 118 mg L^{-1}. (**b**) CYA and DCC decays during anodic oxidation with BDD anode of real swimming pool water with $[CYA]_0$ = 251 mg L^{-1}, at an applied current density of 40 mA cm^{-2}. CYA—filled symbol; DCC—open symbol.

The nitrogen balance supports this interpretation. Nitrate increased from 13 to 75 mg L^{-1} in Sample 1 and from 16 to 97 mg L^{-1} in Sample 2, confirming cleavage of the triazine ring and nitrogen mineralization. At the same time, free and total chlorine rose from undetectable levels to 3–5 mg L^{-1}, indicating that anodic oxidation not only reduces CYA overstabilization but also contributes to the recovery of disinfectant capacity. Free chlorine can also be related to the formation of chloramines, a disinfection by-product formed when chlorine combines with nitrogen-containing compounds, which is considered a less effective disinfectant than chloride and may cause irritation to eyes, skin, and respiratory systems. It is worth noting that, despite the high concentration of CYA in the two studied real swimming pool water matrices, free chlorine values (Table 3) were found to be in the limit regulated by technical-sanitary regulations (5 mg L^{-1}).

The specific energy consumption (SEC) was calculated from the recorded current and cell voltage [25]. Values of 8.3, 27.0, and 33.6 kWh m^{-3} were obtained for current densities of 10, 30, and 40 mA cm^{-2}, respectively, confirming the strong correlation between current density and energy demand. In the second water sample, characterized by higher conductivity, the SEC reached 70 kWh m^{-3} at 40 mA cm^{-2}, mainly due to the extended electrolysis time required to achieve the target degradation. For a broader context, these values can be compared with the study of Long et al. [26], who reported an average electrical energy per order of 117 kWh m^{-3} for the removal of human body fluid pollutants from swimming pool water by EO/UV treatment. This reference illustrates the energy demand expected for complex mixtures of recalcitrant contaminants in similar aquatic environments. In addition, recent pilot-scale work has demonstrated the practical feasibility of electrochemically driven treatments, further highlighting the importance of energy efficiency considerations for scale-up [27].

Concluding, in real swimming pool waters, the lower apparent degradation rate constants observed at higher CYA loads can be explained by the competitive consumption of oxidants by natural organic matter and other background constituents, which delay the oxidation of CYA. Nevertheless, the accumulation of nitrate and the simultaneous increase in free chlorine concentrations demonstrate that the cleavage of the triazine ring proceeds under anodic oxidation and that the process can partially restore disinfectant capacity. In addition, significant TOC removals were observed in both pool water matrices, indicating that the triazine ring was gradually opened and mineralization of organic carbon into CO_2 took place during the AO process.

Finally, accordingly to the measured chemical species detected during the AO-BDD experiments, a reaction pathway is proposed in Figure 9. From these results, it can be concluded that the contribution of mediated oxidation via the chlorine species pathway to the degradation and mineralization of CYA is as relevant as direct oxidation on the BDD surface and hydroxyl radicals in the vicinity of the BDD anode.

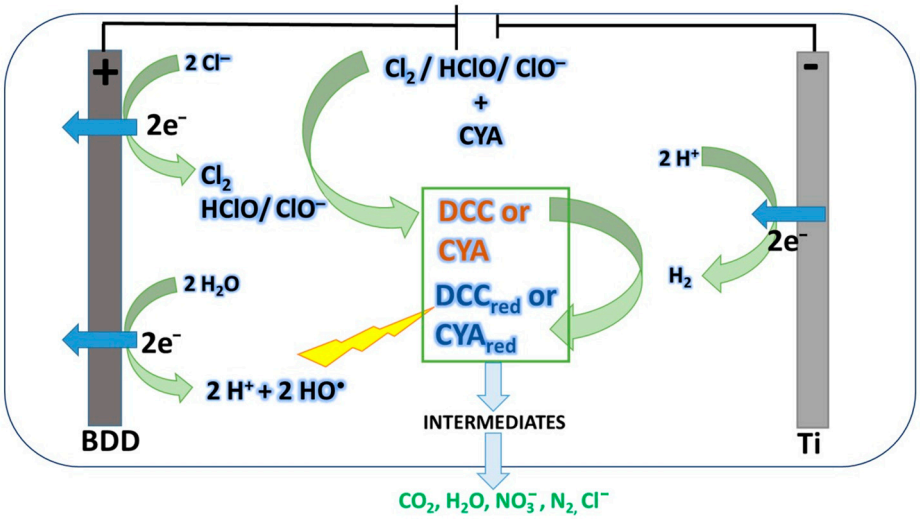


Figure 9. Proposed reaction pathway for CYA degradation during anodic oxidation with BDD electrodes.

4. Conclusions

(1) CYA degradation was evaluated by different AOPs, and AO with BDD anodes showed the highest efficiency, while heterogeneous photocatalysis, photo-Fenton, and photo-persulfate were largely ineffective.

(2) Cyclic voltammetry confirmed that, in the presence of CYA, the oxidation of chloride is delayed, consistent with the formation of organochlorine intermediates.

(3) The effect of operational parameters was systematically studied. Increasing current density enhanced TOC removal and nitrate formation, while TN remained nearly constant, showing that nitrogen is redistributed between organic species and nitrate rather than removed from the system. Higher NaCl concentrations promoted both TOC and TN removal, evidencing the role of active chlorine species.

(4) In real swimming pool water, anodic oxidation with BDD achieved 38% CYA removal in 4 h at 40 mA cm^{-2}, starting from a severely overstabilized matrix (251 mg L^{-1} CYA), without requiring additional electrolyte. This confirms the relevance of the process under realistic conditions.

(5) Overall, the results demonstrate that AO with BDD can effectively control CYA overstabilization while simultaneously regenerating disinfectant capacity, offering a practical alternative to water replacement and avoiding the use of external chemicals.

Author Contributions: Conceptualization, J.C. and J.E.S.; methodology, J.C.; validation, A.F., L.C. and J.A.Z.; formal analysis, J.C. and J.E.S.; investigation, J.C. and I.G.; data curation, J.E.S. and A.L.G.-C.; writing—original draft preparation, J.C., J.E.S. and L.C.; writing—review and editing, A.F. and J.A.Z.; project administration, J.A.C.; funding acquisition, J.A.C. All authors have read and agreed to the published version of the manuscript.

Funding: This research was funded by Fundação para a Ciência e a Tecnologia, FCT, project UIDB/00195/2020 (https://doi.org/10.54499/UIDB/00195/2020) and research contract CEECINST/00016/2021/CP2828/CT0006 awarded to A. Fernandes under the scope of the CEEC Institutional 2021 (https://doi.org/10.54499/CEECINST/00016/2021/CP2828/CT0006); by MINECO PID2019-106884GB-I00; by Ministerio de Ciencia, Innovación y Universidades (MICIU), grant awarded to

J. Carbajo under the Juan de la Cierva_Incorporación program (IJCI-2017-32682); and by CAPES: Science Without Borders Program, Ministry of Education Brazil, grant BEX-1046/13-6 awarded to J. E. Silveira.

Data Availability Statement: The original contributions presented in this study are included in the article. Further inquiries can be directed to the corresponding author.

Acknowledgments: The authors are very grateful for the support granted by the Research Unit of Fiber Materials and Environmental Technologies (FibEnTech-UBI), through the Project reference UIDB/00195/2020, funded by the Fundação para a Ciência e a Tecnologia (FCT), IP/MCTES through national funds (PIDDAC). Furthermore, the authors wish to praise the guidance and helpful collaboration of Ana Lopes, who recently passed away, in this research work and, simultaneously, pay tribute to her for her dedication to the FibEnTech-UBI. Finally, the authors would like to thank Fernando Ruiz-Jarabo for providing real swimming pool water samples with cyanuric acid.

Conflicts of Interest: The authors declare no conflicts of interest. The funders had no role in the design of the study; in the collection, analyses, or interpretation of data; in the writing of the manuscript; or in the decision to publish the results.

Abbreviations

The following abbreviations are used in this manuscript:

AO	Anodic oxidation
BDD	Boron-doped diamond
CYA	Cyanuric acid
DCC	Dichloroisocyanuric acid
DSA	Dimensionally stable anode
HPhCat	Heterogeneous photocatalysis
HPLC	High-performance liquid chromatography
Ph-F	Photo-Fenton
Ph-PS	Photo-persulfate
PS	Persulfate
TN	Total nitrogen
TOC	Total organic carbon

References

1. Adhikary, R.K.; Mahfuj, M.S.E.; Starrs, D.; Croke, B.; Glass, K.; Lal, A. Risk of human illness from recreational exposure to microbial pathogens in freshwater bodies: A systematic review. *Expo. Health* **2022**, *14*, 325–343. Available online: https://link.springer.com/article/10.1007/s12403-021-00447-z (accessed on 7 April 2025). [CrossRef]
2. Chowdhury, S.; Alhooshani, K.; Karanfil, T. Disinfection byproducts in a swimming pool: Occurrences, implications, and future needs. *Water Res.* **2014**, *53*, 68–109. [CrossRef] [PubMed]
3. Teo, T.L.L.; Coleman, H.M.; Khan, S.J. Chemical contaminants in swimming pools: Occurrence, implications and control. *Environ. Int.* **2015**, *76*, 16–31. [CrossRef]
4. Yang, L.; Chen, X.; She, Q.; Cao, G.; Liu, Y.; Chang, V.W.C.; Tang, C.Y. Regulation, formation, exposure, and treatment of disinfection by-products (DBPs) in swimming pool waters: A critical review. *Environ. Int.* **2018**, *121*, 1039–1057. [CrossRef]
5. García-López, E.; Marcí, G.; Serpone, N.; Hidaka, H. Photoassisted oxidation of the recalcitrant cyanuric acid substrate in aqueous ZnO suspensions. *J. Phys. Chem. C* **2007**, *111*, 18025–18032. [CrossRef]
6. Yanagisawa, I.; Oyama, T.; Serpone, N.; Hidaka, H. Successful scission of a recalcitrant triazinic ring. The photoassisted total breakup of cyanuric acid in ozonized TiO_2 aqueous dispersions in the presence of an electron acceptor (H_2O_2). *J. Phys. Chem. C* **2008**, *112*, 18125–18133. [CrossRef]
7. Long, L.; Bu, Y.; Chen, B.; Sadiq, R. Removal of urea from swimming pool water by UV/VUV: The roles of additives, mechanisms, influencing factors, and reaction products. *Water Res.* **2019**, *161*, 89–97. [CrossRef] [PubMed]
8. *Royal Decree 742/2013, 27 September, Establishing the Technical-Sanitary Criteria of Swimming Pools*; Official State Bulletin of the Government of Spain: La Rioja, Spain, 2013; Volume 244, pp. 83123–83135. Available online: https://www.boe.es/eli/es/rd/2013/09/27/742 (accessed on 24 April 2025).

9. Falk, R.A.; Blatchley III, E.R.; Kuechler, T.C.; Meyer, E.M.; Pickens, S.R.; Suppes, L.M. Assessing the impact of cyanuric acid on Bather's risk of gastrointestinal illness at swimming pools. *Water* **2019**, *11*, 1314. [CrossRef]
10. Bobadilla, M.C.; González, E.P.V.; Lorza, R.L.; Gómez, F.S. Effecting partial elimination of isocyanuric acid from swimming pool water systems. *Water* **2019**, *11*, 712. [CrossRef]
11. Oh, Y.-C.; Jenks, W.S. Photocatalytic degradation of a cyanuric acid, a recalcitrant species. *J. Photochem. Photobiol. A Chem.* **2004**, *162*, 323–328. [CrossRef]
12. Abdelli, G.; Leitner, N.K.V. Oxidation of cyanuric acid in aqueous solution by catalytic ozonation. *Ozone Sci. Eng.* **2016**, *38*, 233–241. [CrossRef]
13. Pei, L.Z.; Xie, Y.K.; Pei, Y.Q.; Cai, Z.Y.; Fan, C.G. Determination of cyanuric acid by electrochemical cyclic voltammetry method using $CuGeO_3$ nanowires as modified electrode materials. *J. Nanotechnol. Eng. Med.* **2013**, *4*, 031003. [CrossRef]
14. Chan, C.Y.; Chan, H.S.; Wong, P.K. Integrated photocatalytic-biological treatment of triazine-containing pollutants. *Chemosphere* **2019**, *222*, 371–380. [CrossRef]
15. Mahlalela, L.C.; Casado, C.; Marugan, J.; Septien, S.; Ndlovu, T.; Dlamini, L.N. Photocatalytic degradation of atrazine in aqueous solution using hyperbranched polyethyleneimine templated morphologies of $BiVO_4$ fused with Bi_2O_3. *J. Environ. Chem. Eng.* **2020**, *8*, 104215. [CrossRef]
16. Carbajo, J.; García-Muñoz, P.; Tolosana-Moranchel, A.; Faraldos, M.; Bahamonde, A. Effect of water composition on the photocatalytic removal of pesticides with different TiO_2 catalysts. *Environ. Sci. Pollut. Res.* **2014**, *21*, 12233–12240. [CrossRef] [PubMed]
17. Fernández-Domene, R.M.; Sánchez-Tovar, R.; Lucas-Granados, B.; Muñoz-Portero, M.J.; Garcia-Antón, J. Elimination of pesticide atrazine by photoelectrocatalysis using a photoanode based on WO_3 nanosheets. *Chem. Eng. J.* **2018**, *350*, 1114–1124. [CrossRef]
18. Niu, B.; Cai, J.; Song, W.; Zhao, G. Intermediate accumulation and toxicity reduction during the selective photoelectrochemical process of atrazine in complex water bodies. *Water Res.* **2021**, *205*, 117663. [CrossRef] [PubMed]
19. Yang, N.; Liu, Y.; Zhu, J.; Wang, Z.; Li, J. Study on the efficacy and mechanism of Fe-TiO_2 visible heterogeneous Fenton catalytic degradation of atrazine. *Chemosphere* **2020**, *252*, 126333. [CrossRef]
20. Oturan, N.; Brillas, E.; Oturan, M.A. Unprecedented total mineralization of atrazine and cyanuric acid by anodic oxidation and electro-Fenton with a boron-doped diamond anode. *Environ. Chem. Lett.* **2012**, *10*, 165–170. [CrossRef]
21. Liu, G. Recalcitrance of cyanuric acid to oxidative degradation by OH Radical: Theoretical investigation. *RSC Adv.* **2014**, *70*, 37359–37364. [CrossRef]
22. Malpass, G.R.P.; Salazar-Banda, G.R.; Miwa, D.W.; Machado, S.A.S.; Motheo, A.J. Comparing atrazine and cyanuric acid electro-oxidation on mixed oxide and boron-doped diamond electrodes. *Environ. Technol.* **2013**, *34*, 1043–1051. [CrossRef]
23. Polcaro, A.M.; Vacca, A.; Mascia, M.; Palmas, S. Oxidation at boron-doped diamond electrodes: An effective method to mineralize triazines. *Electrochim. Acta* **2005**, *50*, 1841–1847. [CrossRef]
24. Bensalah, N.; Dbira, S.; Bedoui, A. The contribution of mediated oxidation mechanisms in the electrolytic degradation of cyanuric acid using diamond anodes. *J. Environ. Sci.* **2016**, *45*, 115–123. [CrossRef] [PubMed]
25. Salazar, R.; Brillas, E.; Sirés, I. Finding the best Fe^{2+}/Cu^{2+} combination for the solar photoelectro-Fenton treatment of simulated wastewater containing the industrial textile dye Disperse Blue 3. *Appl. Catal. B Environ.* **2012**, *115–116*, 107–116. [CrossRef]
26. Long, L.; Wang, S.; Gao, Z.; You, S.; Wei, L. Electro-oxidation and UV irradiation coupled method for in-site removing pollutants from human body fluids in swimming pool. *J. Hazard. Mater.* **2024**, *464*, 132963. [CrossRef]
27. Pasciucco, E.; Pasciucco, F.; Castagnoli, A.; Iannelli, R.; Pecorini, I. Removal of heavy metals from dredging marine sediments via electrokinetic hexagonal system: A pilot study in Italy. *Heliyon* **2024**, *10*, e27616. [CrossRef]

Disclaimer/Publisher's Note: The statements, opinions and data contained in all publications are solely those of the individual author(s) and contributor(s) and not of MDPI and/or the editor(s). MDPI and/or the editor(s) disclaim responsibility for any injury to people or property resulting from any ideas, methods, instructions or products referred to in the content.